Title

Luminescence dating of stone wall, tomb and ceramics of Kastrouli (Phokis, Greece) Late Helladic settlement: Case study

Authors

Liritzis, Ioannis
Polymeris, George S
Vafiadou, Asimina
et al.

Publication Date

2019

DOI

10.1016/j.culher.2018.07.009

Peer reviewed

Journal of Cultural Heritage xxx (2018) xxx–xxx

Available online at
ScienceDirect
www.sciencedirect.com

Elsevier Masson France
EM|consulte
www.em-consulte.com/en

Original article

Luminescence dating of stone wall, tomb and ceramics of Kastrouli (Phokis, Greece) Late Helladic settlement: Case study

Ioannis Liritzis[a,*], George S. Polymeris[b], Asimina Vafiadou[a], Athanasios Sideris[a], Thomas E. Levy[c]

[a] University of the Aegean, Department of Mediterranean Studies, Laboratory of Archaeometry, 1 Demokratias Str, Rhodes 85131, Greece
[b] Institute of Nuclear Sciences, Ankara University, 06100 Beşevler, Ankara, Turkey
[c] University of California San Diego, Department of Anthropology, San Diego, USA

ARTICLE INFO

Article history:
Received 31 May 2018
Accepted 11 July 2018
Available online xxx

Keywords:
Mycenaean
Chronology
Late bronze age
Luminescence
Archaeology

ABSTRACT

The Kastrouli Late Helladic (LH) III fortified inland site is located in central Greece between the gulfs of Kirrha and Antikyra, not far from Delphi, controlling the communication between these sites. Characteristic ceramic typology from a tomb and the fortified wall indicate a Late Helladic period (~1300–1100 BC) with apparent elements of reuse of the site in the Geometric, Archaic, Classical and Hellenistic times. The present research refers to the dating by luminescence of the stone wall that circumvents the site, a tomb construction and two ceramics. This approach to applying luminescence dating provides an excellent opportunity to search for the Late Bronze Age (LBA) collapse consequences at the site. The thermoluminescence (TL) measurements of two ceramics were carried out following multiple aliquots made of the polymineral material. For the equivalent dose (ED) estimation of pottery samples, the multiple aliquot, additive dose procedure (MAAD) in TL was applied. Prior to age assessment, the firing temperature was estimated also using TL and it is safe to conclude that the firing temperature of the original ceramic was ca. 400 ± 50 °C. For the case of the rock samples collected from the wall and the tomb, the ED was estimated by applying the Single Aliquot Regenerative OSL (SAR OSL) protocol, after later modifications for polymineralic/mixed quartz-feldspathic samples ('double SAR' protocol). The 'double SAR' protocol procedure includes an infrared stimulated luminescence (IRSL) measurement at 50 °C before the main OSL. Individual ED values ranged between 3.2 to 16 Grays and were accepted based on the following acceptance criteria: recycling ratio between 0.90 and 1.05, recuperation < 10%, dose recovery within ± 10% uncertainties, limited IR response at room temperature, ability to recycle and recover a laboratory attributed dose. For all the measured aliquots, these criteria were fulfilled. Here, six (6) new dates were produced on well stratified archaeological sections and context; two TL dates of ceramics from Tomb A, two OSL dates from stone wall, and two OSL of in situ stone building material from the tomb; the latter four using the surface luminescence dating (SLD). The latter consisted of several aliquots and sub-surface areas making at the end six SLD ages; for the two ceramics TL ages of 890 ± 240 and 1530 ± 290 BC; for the external fortified wall three dates 125 ± 145, 680 ± 130, 437 ± 140 BC and for the tomb 900 ± 138 and 1350 ± 310 BC. The luminescence dating project reconfirms the Late Mycenaean age and reuse of the tomb almost uninterrupted in later periods.

1. Introduction

The Kastrouli Late Helladic (LH) III fortified inland site is located between the gulfs of Kirrha and Antikyra, ca. 7 km southeast of Delphi, controlling the communication between these sites. It dominates a small valley and it was connected to the maritime LH settlements of Vroulia, Steno and Antikyra (Fig. 1a–c; [1]). At least two chamber tombs have been found inside the fortified area, while a number of buildings are identified by geophysical prospection, survey and excavation. The site is important not only for understanding the functioning of smaller settlements in the periphery of the Mycenaean world, but also for establishing the communication, social organization, and trade dynamics between maritime and inland settlements during the LBA in Greece, and in general in the Eastern Mediterranean. It also provides an excellent opportunity to search for the LBA collapse consequences, which seem

* Corresponding author.
E-mail address: liritzis@rhodes.aegean.gr (I. Liritzis).

https://doi.org/10.1016/j.culher.2018.07.009
1296-2074/

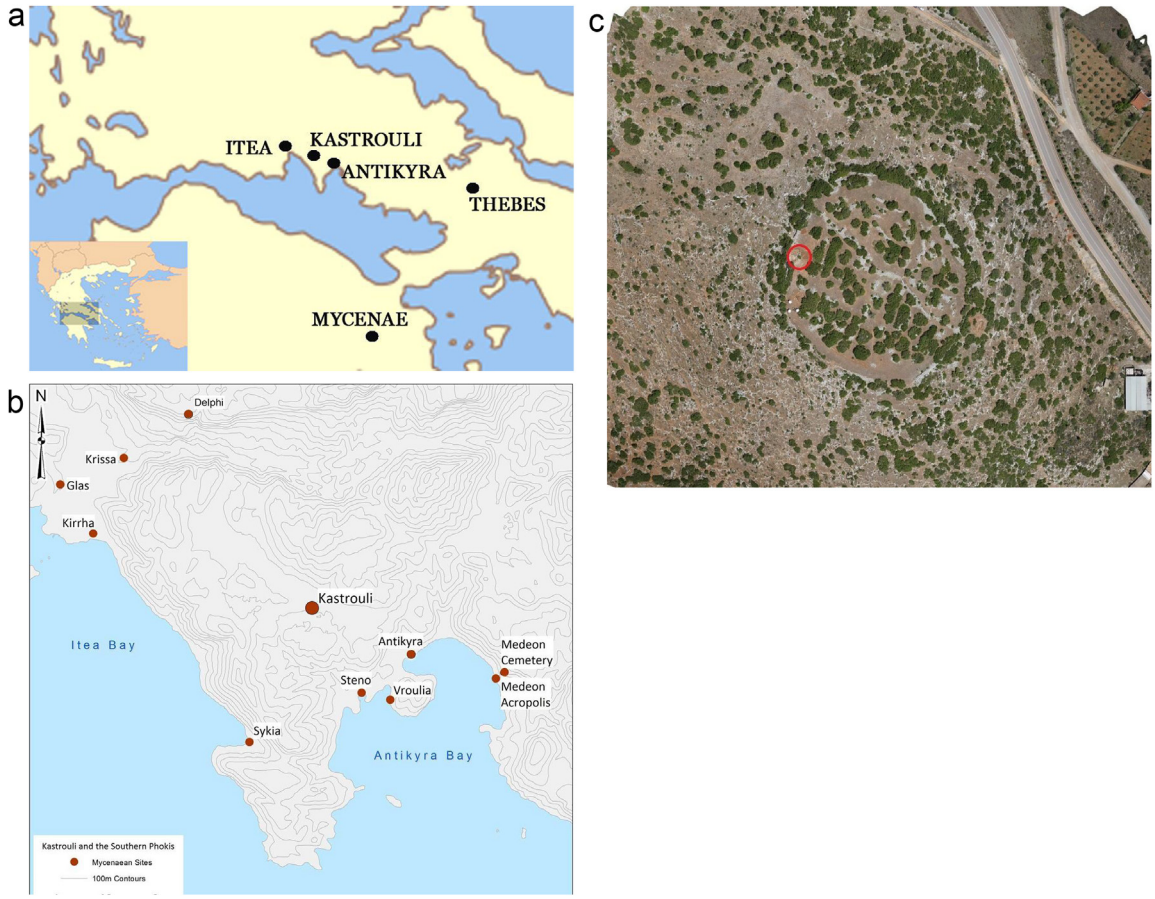

Fig. 1. a: central Greece and Peloponnese. Sites mentioned in the text are shown (Kastrouli, Itea, Antikyra, Mycenae); b: Kastrouli and contemporary coastal sites around the Itea and Antikyra bays; c: aerial view orthophoto from Drone (2.5 cm accuracy) of Kastrouli settlement showing the excavated tomb (red circle).

far less important (if visible at all) among peripheral sites, such as Kastrouli, compared to the core of the Mycenaean world [2].

It has never been explored systematically, but only during summer 2016 a new Project has been initiated by the University of the Aegean (Lab. of Archaeometry & Lab. of Environmental Archaeology) and the University of California San Diego, which funded the excavation [1,3], which continued in 2017 by the University of the Aegean, and from 2018 with University of Brandeis and Wesleyan University from USA. The defensive wall preserved in few courses (max. preserved height 2 m) dates possibly from the Classical period, when Kastrouli was a fort on the boarders between the sacred land, belonging to the Delphic oracle, and the independent city of Antikyra. The sacred land occupied the entire Desfina peninsula and we know its borders only from some Delphic inscriptions of the late Hellenistic and Roman Imperial period [3][3 and references therein], but we can safely assume that the situation has not changed for centuries, and that the inscriptions describing the borders, according the *hieromnemones*, reflect also the situation during the Classical period, or even earlier.

Dasios [4] in his gazetteer of Phokian sites notes for Kastrouli an uninterrupted sequence of pottery from the Mycanaean to the Roman times. The wall was initially supposed to have had only one entrance on its west side, next to a square defense tower, of which only the foundations are preserved [5][5, 1071]. Last season's investigation however revealed a second fortified entrance on the east side of the wall [6][6, forthcoming]. The south wing of the fortification seems earlier, with polygonal masonry and large stones reminiscent of the "Cyclopean" system. At least two tombs were looted between the 1970s to early 1990s. The remnants of pottery, unattractive to the looters, led the first excavator to date the tombs in the LH III B2 period [5][5, 1072]. The recent investigation, however, of tomb A provided proof of a longer period of use [1,3].

A preliminary attempt to date the Kastrouli settlement at Desfina (Delphi Phokis) was made using optical luminescence dating (OSL) on three ceramic and radiocarbon dating (^{14}C) of one bone sample. An initial archaeological reconnaissance of the partially looted site has produced some indication of use during the Late Helladic and later periods. Four ages by luminescence and ^{14}C have shown that this site was used initially in Late Helladic III period, and reused during the Middle Geometric, the Early Archaic and the Classical periods [7].

In this article the objectives are:

- to investigate six (6) dates on well stratified archaeological sections and contexts; two TL dates of ceramics (Fig. 2) from Tomb A, two OSL dates from stone wall (Fig. 3) on the entrance on its west side, and two OSL from stone associated with the tomb construction; the latter four using the surface luminescence dating;
- searching for the Late Bronze Age collapse consequences at the site.

2. Samples, sampling and handling

The stone samples were of limestone (Mg-C) with traces of quartz confirmed by XRD. They were taken from closely joined carved cobbles of foundation wall and the building carved rocks of a tomb with the aid of a hammer and chisel, exerting care to remove pieces of around 2 × 2 cm, preserving the original surface (Fig. 3). Samples were swiftly wrapped in black plastic bags in order to avoid

Please cite this article in press as: I. Liritzis, et al., Luminescence dating of stone wall, tomb and ceramics of Kastrouli (Phokis, Greece) Late Helladic settlement: Case study, Journal of Cultural Heritage (2018), https://doi.org/10.1016/j.culher.2018.07.009

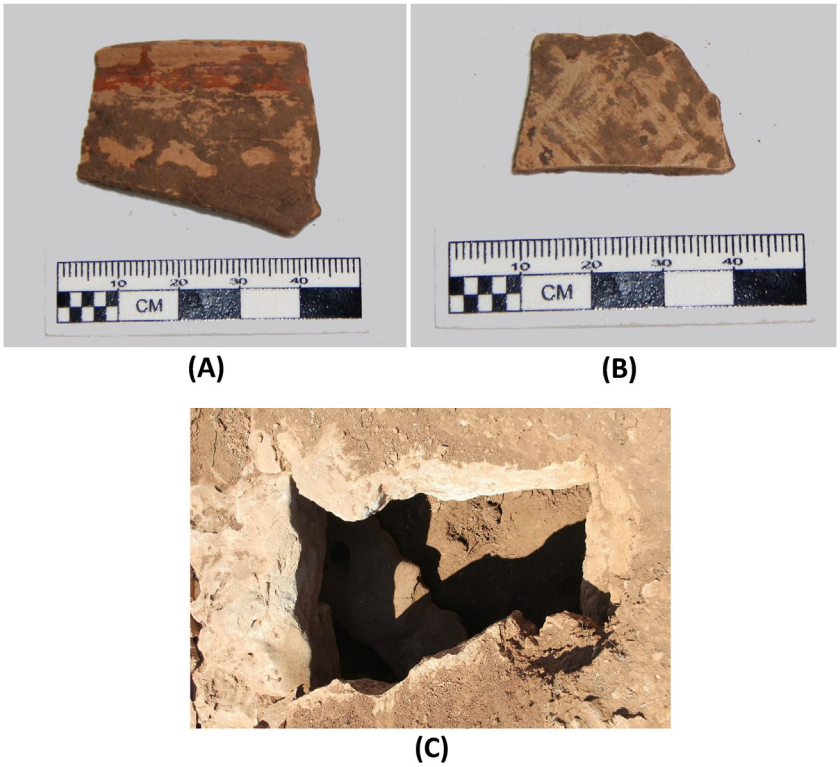

Fig. 2. The two ceramics (A) diagnostic, (B) non diagnostic and (C) locus 110.

exposure to light. As an added precaution against light exposure, the sampling took place late in the evening while the adherent soil on the surface helped to prevent sunlight from reaching the surface [8–11]. The surface's exposure time to sunlight depends on the time taken by the stonemasons to put a given block in the appropriate position overlaid by another. From the moment that any surface is no longer exposed to sunlight and put in firm contact with mortar, the luminescence signal starts to develop.

The original surface of the sample was cleaned, under red-light conditions, with diluted HCl acid to remove dust, and any organic residues and secondary salt by-products. A gentle removal of a ~50 μm layer is made by a fast immersion to diluted HCl, repeated around five times [10]. Fine powder sample is finally removed through a gentle rubbing of ×50 traverses of surface. A thin layer of surface powder was acquired by gently scraping the inter-block surface to a depth of less than 0.5 mm (making a series of readings with a micrometer) and transferred to an acetone bath where grains were collected, washed in dilute acetic acid (0.5%) for 1 min, and left to dry overnight in an oven at 50 °C. TL measurements were carried out following multiple aliquots made of the polymineral material on which the total bleach assumption was applied, which is only valid for cases where here the sample has been exposed to sunlight for a long duration. Fine grains of bi-mineral mix of calcium carbonate with quartz were acquired (polymineral fine grains), as XRD has shown, for further OSL measurements. In fact, 9-mm-diameter discs made of a 0.5-mm-thick aluminum substrate, each one containing ~2 mg of the sample (depending on the availability), were prepared. In all rock samples the powder acquisition surface was divided into sub-areas, i.e. in the unexposed surface, the acquisition of powder came from 4–5 aliquots This sub-area sampling is made to check possible destruction due to pressure/friction (earthquakes) or powder acquisition of visually unnoticed removed surface flake during sampling of parts of surface that may lead to an overestimated geological dose. Indeed, the two carved blocks are not usually overlapping on their entire flat face, and any exerted pressure may cause friction in some parts, not in all, of the contact surfaces [10]. The handling procedure of the pottery samples included the following steps:

- removal of the outer 5-mm thick layer of the pottery samples, in order to eliminate the light-subjected parts of the samples;
- gently crushing in an agate pestle and mortar;
- extraction of grains within the grain size range 4–12 μm;
- suspension in acetone and final precipitation onto 1-cm diameter aluminium discs [12].

The two ceramics derive from Locus 110 which was initially opened beneath the collapsed lintel stone (the stone that we needed the ropes to remove) in the tomb to excavate the sediment beneath it (Fig. 4). Once the sediment was removed, and the area beneath the stone was level with the rest of the tomb, locus 110 was extended to encompass the entire interior of the tomb (below locus 107 and 108). Locus 110 was excavated down to bed rock in the central portions of the tomb, but was closed when the vertical stone slab was discovered at the eastern end of the tomb (by the burials). Also, a modern safety pin was found in sieve from locus 110, indicating that this stratum was disturbed by the looters [1,3]. These two sherds were found amongst debris that may have derived from surrounding surface fill, or they may have belonged to the disturbed grave offerings.

3. Luminescence dating instrumentation and protocols

3.1. Dating instrumentation

Luminescence measurements were performed using a RISØ TL/OSL reader (model TL/OSL – DA – 15), equipped with a high-power blue LED light source, an infrared solid state laser and a 4.5 Gy/min $^{90}Sr/^{90}Y$ β-ray source [13]. The reader is fitted with a 9635QA PM Tube. All TL measurements were carried out in a nitro-

Please cite this article in press as: I. Liritzis, et al., Luminescence dating of stone wall, tomb and ceramics of Kastrouli (Phokis, Greece) Late Helladic settlement: Case study, Journal of Cultural Heritage (2018), https://doi.org/10.1016/j.culher.2018.07.009

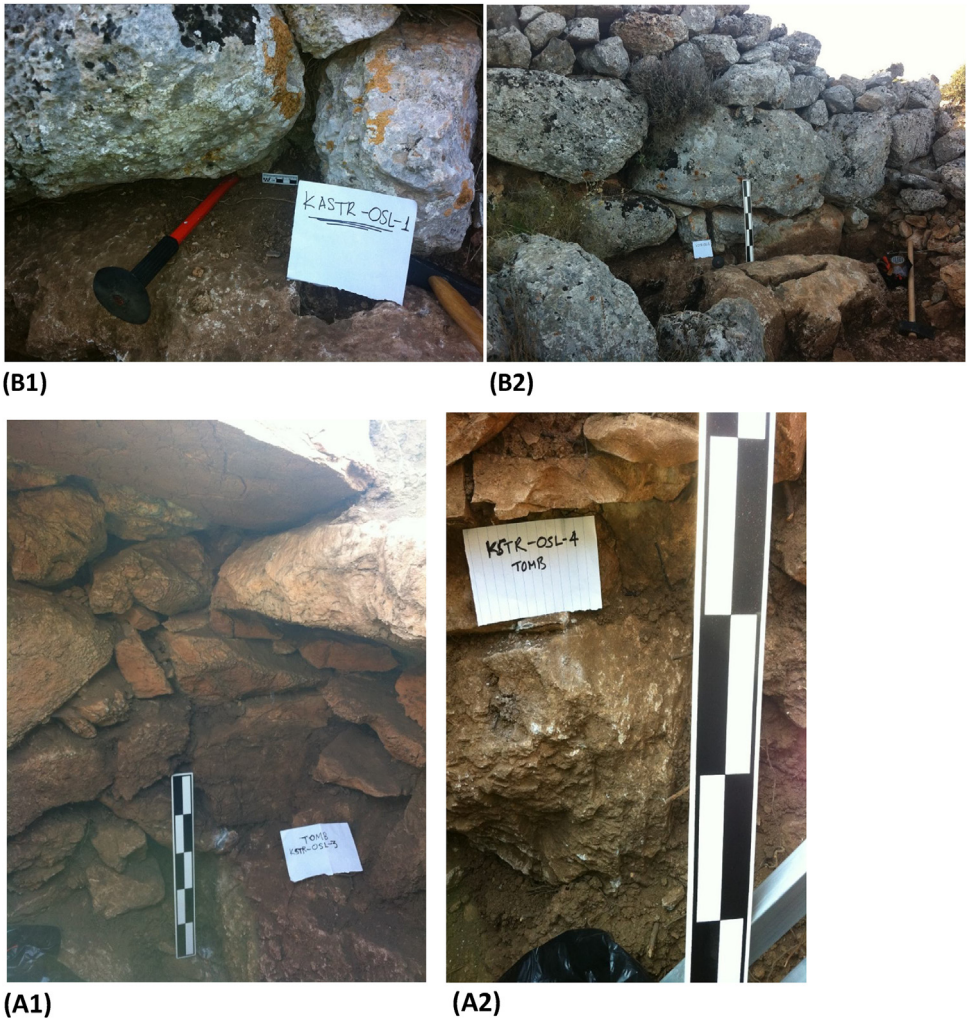

Fig. 3. Sampling from a1–2) the tomb, and, b1–2) the fortified wall.

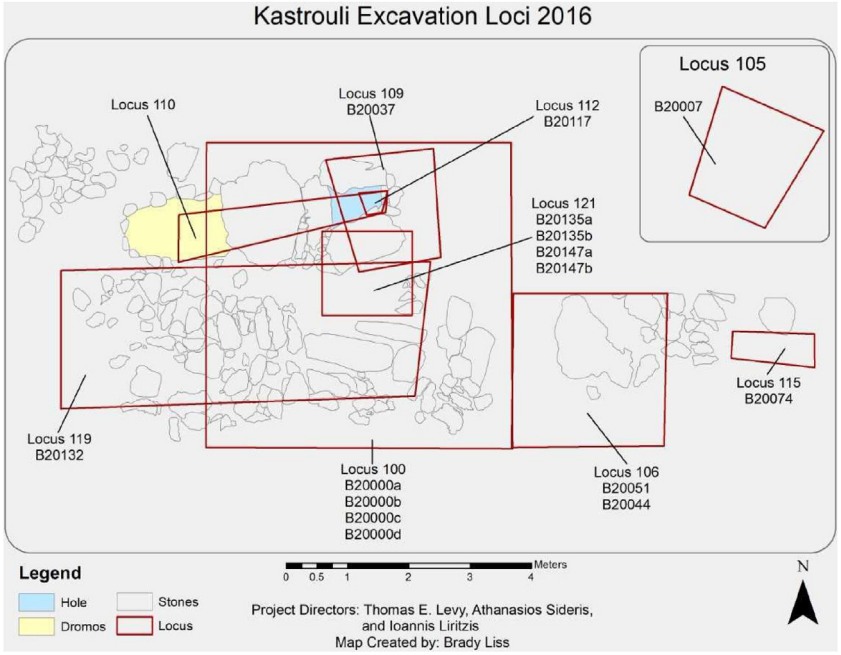

Fig. 4. Locus of excavated ceramics at Kastrouli (Map by Brady Liss, UC San Diego Levanine Archaeology Laboratory).

Please cite this article in press as: I. Liritzis, et al., Luminescence dating of stone wall, tomb and ceramics of Kastrouli (Phokis, Greece) Late Helladic settlement: Case study, Journal of Cultural Heritage (2018), https://doi.org/10.1016/j.culher.2018.07.009

gen atmosphere using a slow heating rate of 2 °C/s, in order to avoid significant temperature lag [14], up to the maximum temperature of 500 °C. For the TL measurements the detection optics consisted of a combination of a Pilkington HA-3 heat absorbing and a Corning 7–59 (320–440 nm) filter. OSL measurements were performed using a 7.5 mm Hoya U-340 (λp ~ 340 nm, FWHM 80 nm) filter, transmitting in the 280–380-nm region, with maximum transmittance (57%) at 330 nm. Blue light-emitting diodes (LEDs, 470 ± 30 nm) were used for OSL stimulation; the power level was software controlled and set at 90% of the maximum power of the blue – LED array, delivering at the sample position ~ 32 mW·cm^{-2}. All OSL measurements were performed at the continuous wave configuration (CW-OSL), for 100 s at 125 °C. For infrared laser stimulation (IRSL), the stimulation wavelength is 875 (± 40) nm and the maximum power is ~ 135 mW/cm^2. All (pre) heatings were performed in a nitrogen atmosphere using a slow heating rate of 1 °C/s, similar to the case of TL measurements. The quartz grains were mounted on stainless steel disks using silicon spray. Regardless of the luminescence protocol applied for all samples, typical treatment and preparation were undertaken, in subdued red filtered light conditions.

The a-counter used for the specific measurements is the ELSEC Low Level Alpha-Counter 7286 with an EMI 6097BPM tube, and ZnS(Ag) on mylar film, incorporating an internal 6502 microprocessor [10,15,16].

3.2. Luminescence protocols

Equivalent doses: for the equivalent dose (ED hereafter) estimation of pottery samples, the multiple aliquot, additive dose procedure (MAAD) in TL was applied; the procedure is described thoroughly by Aitken [15], Wagner [17] and Liritzis et al. [9]. In the framework of this technique, each one of the pottery samples was divided into 18 separate discs-aliquots and independently irradiated to regenerate an individual TL glow curve. Mass reproducibility for all discs-aliquots was kept within ± 3%. For each pottery sample, discs were irradiated in groups of four discs at each dose; only for the group of natural TL six aliquots were used. Three artificial doses of 10, 20 and 30 Gy were attributed, plus a zero Gy additive dose, corresponding to the natural TL (NTL hereafter) signal. A background signal measurement, also known as reheat, was measured for each aliquot and thus subtracted from each glow curve. To the group of aliquots that were used for measuring the NTL levels, subsequently a low dose was applied to each aliquot, in order to check for supralinearity corrections (I). The doses applied were 1.25, 2.5, 3.75, 5, 6.25 and 7.5 Gy; each dose was attributed to one disc-aliquot.

For the case of the rock samples collected from the wall and the tomb, the ED was estimated by applying the Single Aliquot Regenerative OSL (SAR OSL) protocol [18], after the modifications suggested by Banerjee et al. [19] for polymineralic/mixed quartz-feldspathic samples ('double SAR' protocol). The 'double SAR' protocol procedure includes an infrared stimulated luminescence (IRSL) measurement at 50 °C before the main OSL, permitting thus the separation of the signal resulting from feldspars and quartz. Fine grains were used and quartz in limestone was measured [20]. The protocol applied includes the following steps Table 1.

Regeneration doses were chosen in order to bracket the equivalent dose. The equivalent dose was then estimated as the dose required producing the natural signal, by interpolating it from the corrected growth curve. The latter was modelled for each aliquot by a linear growth form. The background OSL levels measured after 98–100 s exposure were subtracted from the initial luminescence intensity (signal integrated over the first stimulation s) of the decay curves obtained.

Table 1
The Double SAR protocol applied in the framework of the present study. Regeneration doses include 0 (NOSL), 0.5 Gy, 1.2 Gy, 1.7 Gy, 3.5 Gy, 6 Gy, 11 Gy, 0 Gy (recuperation point) Gy, 1.7 Gy (recycle point).

Protocol
Step 1: dose
Step 2: preheat 200 °C
Step 3: IRSL, 50 °C, 100 s
Step 4: OSL, 110 °C, 100 s
Step 5: test dose (1.2 Gy)
Step 6: cut heat 180 °C
Step 7: IRSL, 50 °C, 100 s
Step 8: OSL, 110 °C, 100 s

3.3. Firing temperature assessment

Each ceramic sample was divided into nine segments. Each segment was annealed (re-fired) to a different temperature between 100 °C and 900 °C, in steps of 100 °C in order to bracket the firing temperature. Each annealing was followed by fast cooling to room temperature. After the annealing, each segment was crushed and grains of dimensions 90–180 μm were selected and deposited on aluminium cups of 1 cm^2 area; the specific grain size fraction was selected based on the suggestion of Polymeris et al. [21]. Mass reproducibility throughout the entire annealing temperature region was kept within 3–5%. Subsequently, the initial sensitivity, as well as the pre-dose sensitization was recorded for both the 110 °C TL peak as well as the rest of the TL glow curve as a function of the annealing temperature. This is the protocol suggested by Polymeris et al. [21,22] and further applied to a number of case studies [21,23,24]. The test dose applied was 10 Gy Table 2.

4. Luminescence results

4.1. TL of ceramics

Fig. 5a presents typical TL glow curves of the additive dose procedure for sample RHO-1156. The NTL signal consists of two prominent TL peaks, centred at 275 and 330 °C; the same TL peaks are also observed in the natural plus additive TL glow curves, among others. It is worth noticing that, even though reheats (or alternatively background curves) were subtracted, the glow curves yield the presence of an increasing part after 425 °C, corresponding to deeper traps, with delocalization temperature above 500 °C; these are also known as very deep traps (VDT) in the literature [25]. Similar glow curve shape was observed for the other sample as well. Fig. 5b presents a representative NTL + β-dose response curve for the sample RHO-1156. In this latter plot, additive dose measurements are presented as squares, while the second glow TL measurements, which were performed for checking the supralinearity index (I) and the corresponding correction, are presented as dots. Both TL dose response curves presented in Fig. 5b correspond to temperature of 320 °C. Arrows in the figure indicate

Table 2
A summary of the TL data required for age and firing temperature assessment of the pottery samples. Numbers in parenthesis indicate the corresponding errors.

Name	ED (Gy)	ΔT plateau (°C)	I (Gy)	ED + I (Gy)	Firing T (°C)
RHO-1156, ceramic 1	11.88 (0.75)	290–375	3.39 (0.43)	15.27 (1.18)	400 (50)
RHO-1157, ceramic 2	13.51 (0.87)	275–355	2.68 (0.39)	16.19 (1.26)	–

Please cite this article in press as: I. Liritzis, et al., Luminescence dating of stone wall, tomb and ceramics of Kastrouli (Phokis, Greece) Late Helladic settlement: Case study, Journal of Cultural Heritage (2018), https://doi.org/10.1016/j.culher.2018.07.009

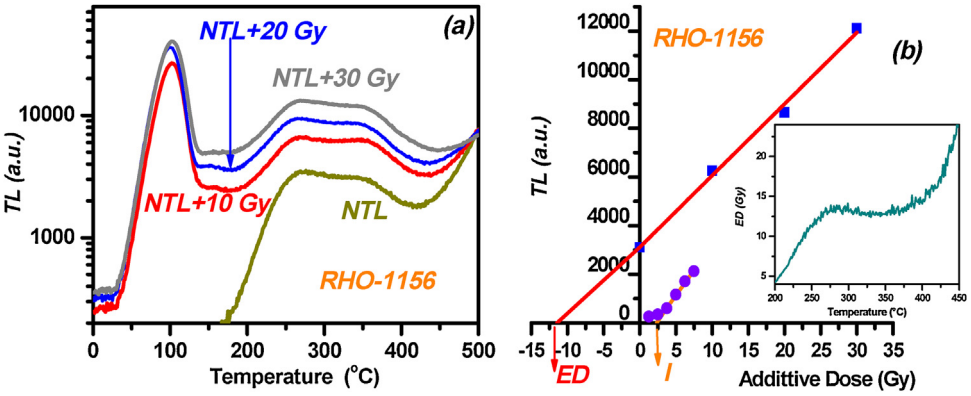

Fig. 5. Plot (a) presents natural (yellow curve) and natural plus-beta dose glow curves in the framework of the TL MAAD technique applied. The additive doses delivered were 10 (red curve), 20 (blue curve), and 30 Gy (grey curve). Reheats have been subtracted. The plotted natural thermoluminescence (NTL) is the average of five individually measured NTLs. NTL-plus-beta glow curves are the averages of three or four individually measured glow curves. Plot (b) presents a representative NTL + β-dose response curve for the temperature of 320 °C; additive dose measurements (squares) as well as second glow measurements (dots) for the supralinearity correction. Arrows indicate the ED and I, respectively. Inset presents the best equivalent dose plateau plotted versus the glow curve temperature.

the ED and I, respectively. ED values were calculated over a wide temperature region, according to the following equation 1 [11]:

$$\mathrm{ED} = \frac{\frac{NTL(T)}{[(NTL+\beta_i)(T)-NTL(T)]}}{\beta_i}(Gy) \quad (1)$$

where (NTL + β_i) denotes the corresponding glow curves after the corresponding additive dose has been administered, so the preceding subtraction takes place for each data point. The denominator strongly establishes the linearity of the additive dose response [26] over quite an extended range of glow curve temperatures, despite the relatively large additive doses used. Only linear fittings were applied for the ED calculation. A typical plot of ED against glow curve temperature is presented in the inset of Fig. 5b. Wide equivalent dose plateaus were yielded, with the equivalent doses being obtained as the mean values of the best plateaus for each sample. Errors derived mainly from the uncertainties in curve fitting, are ± 1σ and were calculated by standard error propagation analysis. A summary of the TL data is given in Tables 3 and 4.

4.2. OSL of stones

Despite the relatively poor intensity of (mostly) the natural OSL signals, all signals yield the presence of a convenient fast OSL component, which depletes within 5–10 s of stimulation. Therefore, the use of the initial signal intensity, integrated over the first stimulation s of the decay curves, is justified. Individual ED values were accepted based on the following acceptance criteria: recycling ratio between 0.90 and 1.05, recuperation < 10%, dose recovery within ± 10% uncertainties, limited IR response at room temperature, ability to recycle and recover a laboratory attributed dose. For all the measured aliquots, these criteria were fulfilled. The individual ED values obtained are presented in Table 4. The credibility of these ED values is strongly supported by the values of both the recycling ratios of the main measurements (naturally accrued dose), which lie within the range 0.93–0.99, and the recuperation, which is less than 8.1%; these afore mentioned values, are also presented in Table 3. The successful application of the applied protocol with the specific corresponding parameters, such as the preheating and cut heat temperatures as well as the regenerative doses applied, was further checked by a dose recovery test according to Murray and Wintle [27]. Due to the restricted amount of sample, a limited number of aliquots were put aside, in order to perform the dose recovery test, which includes two room temperature optical stimulations for 150 s, in order to bleach the aliquots, with a 10-ks room temperature storage in between. Afterwards, each sample was given a laboratory β-dose, selected to be of the same order of magnitude as the equivalent dose estimated by the double SAR analysis. This dose was further treated as an unknown, and the same double SAR protocol of Table 1, was then applied by using the same given β-doses and measuring parameters. Dose recovery results indicated that for all aliquots, the ratio of the measured to given dose is within ~ 13% of unity, indicating the suitability of the specified SAR procedure to recover successfully the given β-dose delivered to the samples.

4.3. Firing temperature of ceramics

The underlying idea of the quartz glow curve sensitization method for the firing temperature assessment is that thermally induced hole transfer of charge associated with geological irradiation takes place during firing, and the re-firing experiments can reconstruct the point at which additional sensitization takes place [24]. The sensitization of the glow curve of quartz occurs within the temperature range between 200 °C and 900 °C. Temperatures above are excluded, since these can cause vitrification. Once a quartz sample is annealed (or re-fired) to a temperature that is higher than these that corresponds to the firing of original pottery sample (from which the quartz was extracted) a sensitization of the 110 °C peak is observed [28].

The glow curves obtained within the framework of the protocol for the assessment of the firing temperatures yield shapes identical with the NTL + β_i glow curves of Fig. 5a. For this reason, these glow curves are not presented. Fig. 6 presents the normalised intensity, due to re-firing, of (a) only the 110 °C TL peak (dots) and (b) the rest of the TL glow curve (squares) versus re-firing temperature. For the former case, the normalised sensitivity is stable up to 400 °C, while for temperatures above a sharp increase is monitored. For the rest of the glow curve, a mild decrease is monitored within the temperature range between 100 and 400 °C; this mild decrease could be attributed to the partial zeroing of the NTL signal due to the annealing. Nevertheless, after 400 °C, the intensity of the rest TL glow curve also increases steeply. Similar results were also monitored for the pre-dose sensitization of the corresponding signals. Based on the results presented in Fig. 6, it is safe to conclude that the firing temperature of the original ceramic is 400 °C. This value stands in very good agreement with the presence of VDT, namely NTL signal for glow curve temperatures above 425 °C. As the experiments were performed in steps of 100 °C, it is safe to indicate that the error for this aforementioned assessment is 50 °C. Finally, it is worth mentioning that the technique works only for one ceramic sample. For

Table 3
Individual and average OSL data required for age assessment for stones (wall and tomb).

Name	Aliquot/average	ED (Gy)	Recycling ratio	Recuperation (%)
RHO-1161-1	1	3.37 (0.27)	0.95	5.6
RHO-1161-1	2	3.31 (0.24)	0.94	6.1
RHO-1161-1	3	2.93 (0.18)	0.94	5.8
RHO-1161-1	4	3.15 (0.21)	0.96	7.3
RHO-1161-1	***Average***	***3.19 (0.19)***	***0.95 (0.01)***	***6.2 (0.8)***
RHO-1161-2	1	4.16 (0.29)	0.93	7.6
RHO-1161-2	2	4.06 (0.25)	0.93	8.1
RHO-1161-2	3	3.98 (0.23)	0.94	6.8
RHO-1161-2	4	3.85 (0.24)	0.95	7.6
RHO-1161-2	***Average***	***4.02 (0.14)***	***0.94 (0.01)***	***7.5 (0.6)***
RHO-1162	1	3.78 (0.22)	0.96	4.3
RHO-1162	2	3.49 (0.21)	0.94	7.1
RHO-1162	3	3.61 (0.23)	0.97	7.9
RHO-1162	4	3.85 (0.23)	0.97	6.2
RHO-1162 wall kastr-2	***Average***	***3.68 (0.17)***	***0.96 (0.02)***	***6.5 (1.5)***
RHO-1163	1	4.78 (0.35)	0.99	3.9
RHO-1163	2	5.12 (0.41)	0.97	4.1
RHO-1163	3	4.69 (0.34)	0.98	4.9
RHO-1163	4	4.81 (0.37)	0.97	4.2
RHO-1163	5	4.99 (0.39)	0.99	5.7
RHO-1163	***Average***	***4.88 (0.18)***	***0.98 (0.01)***	***4.6 (0.9)***
RHO-1164	1	5.35 (0.44)	0.96	6.2
RHO-1164	2	6.28 (0.52)	0.99	5.4
RHO-1164	3	5.96 (0.54)	0.97	4.4
RHO-1164	4	4.97 (0.39)	0.95	6.9
RHO-1164	5	6.11 (0.49)	0.98	5.2
RHO-1164 tomb kastr-4	***Average***	***5.73 (0.51)***	***0.97 (0.02)***	***5.5 (0.7)***

For each individual value the value in parenthesis indicates the corresponding estimated error. In bold and italics, the average values along with the corresponding standard deviations. For individual recycling ration value, an error of 0.05 is assigned. Recuperation is calculated in terms of percentage over the corresponding equivalent dose.

Table 4
Samples and sample location, dose rates by alpha counting and XRF, total equivalent doses, dose rates and deduced ages.

Code sample/location	U (ppm)	Th (ppm)	K (%)	Rb (ppm)[e]	Water UPTAKE (%)	Dose rate, mGy/yr	Total dose, Gy	Age, years BC
RHO-1161 (KASTR-OSL-1) NW fortified Wall	2.59 (0.1)	0.34 (0.19)	0.04 (0.002)	0	60[a]	1.50 (0.05)[b]	3.19 (0.19) 4.02 (0.14)	125 ± 145 680 ± 130
RHO-1162 (KSTR-OSL-2) NW fortified Wall (another part is 1161)	2.59 ± 0.10	0.34 ± 0.19	0.12 (0.05)	6	60 (+10/−20)	1.51(0.05)[b]	3.68(0.17)	437 ± 140
RHO-1163 (KSTR-OSL-3) Tomb western side (same rock as 1164)	0.71 ± 0.04	0.06 ± 0.07	0.06 (0.002)	3	60	1.68 (0.05)[d]	4.88 (0.18)	900 ± 138
RHO-1164 (KSTR-OSL-4) Tomb Eastern side	0.71 ± 0.04	0.06 ± 0.07	0.06 (0.002)	3	60	1.71 (0.05)	5.73(0.51)	1350 ± 310
RHO-1158 (infill mortar, sediment) samples 1 and 2 (for 1161, 1162)	4.93 ± 0.20	6.96 ± 0.48	2.32 (0.1)	89	30 ± 20	–	–	–
RHO-1159 (infill mortar, sediment) sample 3 (tomb west side)	4.38 ± 0.23	8.98 ± 0.69	2.58 (0.11)	112	30 ± 20	–	–	–
RHO-1160 (infill mortar, sediment) sample 4 (tomb east side)	4.31 ± 0.24	10.32 ± 0.78	2.66 (0.12)	108	30 ± 20	–	–	–
RHO-1156 (KAS-C1) diagnostic ceramics	4.22 ± 0.42	15.22 ± 1.50	3.18 (0.14)	110	60	5.28[c] (0.14)	15.27 (1.18)	890 ± 240
RHO-1157, ceramic non diagnosed	6.71 ± 0.43	10.80 ± 1.20	1.87 (0.06)	65	60	4.58[c] (0.10)	16.19 (1.26)	1530 ± 290
RHO-1165, surface soil (Liritzis et al., 2016)	4.78 ± 0.18	10.70 ± 0.80	2.40 (0.11)	100	60	–	–	–

[a] The water uptake for the mortar is accepted as 30% and for the sediment 60%.

[b] The gamma ray dose rate for the wall and the tomb samples derive 3/4th from the surrounding rock wall; 1/4th from sediment with water uptake 60% which attenuated through ~20 cm sediment and due to 60% water uptake becomes 0.04 mGy/yr (see [3] below). For the Db half of the rock beta is taken as no obvious mortar was between the boulders.

[c] The DR comprises of the alphas, betas from the ceramic itself and the environmental gammas. The Dg, soil, wet is 1.34 ± 0.04, and the surface soil was diluted from debris of pebbles and ceramics while the background was rocky local limestone made flat. The average soil thickness was 20 cm that provides for a sherd on half this layer 35% = 0.47 mGy/yr. (see eq. in the text). In addition to that the rock background provides another gamma dose which amounts to about 1/2nd. Thus, Dg of stone tomb and wall of 0.25 mGy/yr half of this attenuated through ~20 cm soil and due water uptake soil becomes 0.08 mGy/yr which corresponds to ceramics. In addition, the cosmic ray dose rate 0.20 and the internal quartz dose rate 0.1 mGy/yr.

[d] The RHO-1163 (1.67 mGy/yr) and RHO-1164 (1.71 mGy/yr) rock samples from the tomb have slight different radioisotopic content than the RHO-1161 and RHO-1162 from the external fortified wall samples, the radiation geometry however is accepted a little higher than those. Derived from the near the basement of the side wall of the tomb in a confined space (80%Dg); while the little sediment there would amount 0.08 mGy/yr (see [1] above; there was observed mortar between the boulders thus Db is taken half of the measured infill mortar.

[e] K/Rb = 200, 0.0185 mGy/yr = 50 ppm [35].

Please cite this article in press as: I. Liritzis, et al., Luminescence dating of stone wall, tomb and ceramics of Kastrouli (Phokis, Greece) Late Helladic settlement: Case study, Journal of Cultural Heritage (2018), https://doi.org/10.1016/j.culher.2018.07.009

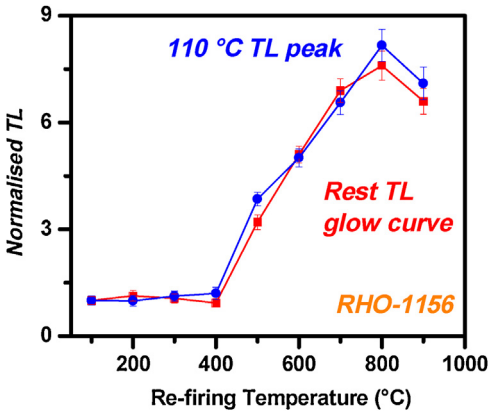

Fig. 6. The normalized TL sensitivity versus re-firing temperatures corresponding to the 110 °C TL peak (points) as well as the rest of the higher glow peaks of the glow curve (squares) for the sample with code name RHO-1156. Normalization has been carried out over the respective first data point corresponding to the re-firing temperature of 100 °C. The plots represent re-firing sensitization. Similar results were also yielded for the pre-dose sensitization. Based on the rationale presented above, firing temperature was estimated to be 400 °C.

the other ceramic sample, a firing at a temperature higher than 800–900 °C, which does not cause vitrification, might be possible. Firing at higher temperature has been observed to destroy the radiation sensitive traps and create thermally sensitive traps while, on the contrary, the growth defects disappear after prolonged irradiation. According to Koul [29], this sort of transformation is primarily activated by the kinetics of the monovalent alkali ions, the switch over of which has a key role in influencing the utility of the TL sensitivity of the 110 °C peak to monitor the firing temperature. The results are also presented in Table 2. For an outline regarding the limitations on the technique, the readers could refer to Polymeris et al. [21] as well as to Sanjurjo-Sanchez et al. [24].

4.4. Dose rates

The results for the annual dose rate measurements for all the samples and the surrounding soil and the total Dose Rate estimation for the samples are summarized in Table 4. The value of the alphas/betas efficiency was adopted to be 0.1 [30], the cosmic ray dose rate of 0.20 mGy/yr (estimated as per Prescott and Hutton [31]), the internal quartz dose rate 0.1 mGy/yr is assumed; finally, for the overlaid stones, half the beta dose rate is considered, because a surface layer of about 50 μm is removed by diluted acid, and due to the thin layer of paste between them, only the beta particles from the lower (sampled) block are accounted for. Dose rates ranged from 1.50 for stones to 5.8 for ceramics in mGy/yr. A similar result was deduced from calculations of individual radiation components of cosmic plus the rock plus the ground soil of the almost 2 π counting geometry. The Rb value was estimated by the ratio Rb/K = 1/200; water uptake is taken 60% from data of the National Meteorological Service for the period 1961–2018.

Potassium and other oxides were measured using scanning electron microscopy (SEM) measurements coupled with an energy dispersive spectrometer (EDS) (Philips FEI-Quanta INSPECT with SUTW detector) at the Laboratory of Archaeometry of the Department of History, Archeology, and Cultural Resources Management, University of Peloponnese, Greece).

Concerning the environmental gamma ray dose rate the radiation geometry per sample is complicated and needs special attention. The ground soil was diluted from debris of pebbles and ceramics while the background was rocky local limestone made flat. The average soil thickness was 20 cm that provides for a sherd on half this layer 35% $D_{g,wet,inf}$ of 1.34 or 0.47 mGy/yr (see Table 4) for average photon energy E = 1.5 MeV and density 1.65 g/cm^3. The overlapping media of bedrock and soil much like discs (in cylindrical forms) were converted into spheres of equivalent volume with corresponding radius values. An estimation of fraction F of infinite matrix gamma dose rate expected at the center of radius r, was derived from equation 2:

$$F = 1 - e^{-\mu_o \cdot r}\,[1 + (\mu_o - \mu_a).r]$$

μ_o is the linear attenuation coefficient and μ_a the linear absorption coefficient (taken from Storm and Israel [32] and Evans [33]) for densities 1.6 g/cm^3, r the radius of the soil medium. The $\mu = \rho\,\Sigma(\mu_i/\rho_i)\omega_i$, ρ the measured density of the matrix and the summation is taken over the i constituents of the matrix according to their fraction by weight ω_i (air space and water are ignored). The equation is based on theoretical considerations by Evans [34]. The alpha and beta radiation from U, Th, K deposit their energy along their track into the grain size, reduced by an attenuation factor. The water uptake for the site is estimated as 60% throughout the year and the corrected Di, for alpha, beta and gamma dose rate from the dry infinite gamma dose rate $D_{i,d}$ is $D_{i,w} = D_{g,d}/(\lambda[1.5–1] + 1)$, where λ is 1.50, 1.25, 1.14 respectively for alphas, betas and gammas.

The dose rates, the ED the radioisotopic content and the obtained ages and associated errors are given in Table 4; the ages span a millennium from the Hellenistic era to Late Helladic times. The conversion of U, Th, K, Rb isotopic concentration to dose rates was based in Liritzis et al [35].

5. Discussion

Pottery and figurines datable on typological and stylistic criteria from the Tomb A range from LH III A2 to LH III C Early or Developed ([3], 278–279). There is no doubt that the Tomb A was used during a long period, a fact confirmed moreover by a large comingled burial that included at least nineteen individuals identified by the biological anthropology study of the skeletal remains [36]. Although the absolute chronology is still debated for the Late Helladic period [37–41], it seems relatively safe to ascribe the pottery and the figurines from the Tomb A to various dates between 1370 and 1090 BC (longest possible time-range) or between 1320 and 1170 BC (shortest possible time-range). One hundred and fifty years was thus, the shortest possible period during which the Tomb A has been in continuous use. The two ceramics TL ages are 890 ± 240 and 1530 ± 290 BC. There is no problem with the higher date, which overlaps with the typological dates for 80 years minimum or for 130 years maximum. The lower ceramic TL date, however, indicates that we should opt for the use of the Tomb A at least until 1120/10 BC, invalidating thus the higher typological/stylistic date of 1170 BC as latest date for the use of the tomb. The maximum overlap that we may obtain between typological pottery dates and the lower TL date for the use of the Tomb A is barely 40 years. In conclusion, the combination of stylistic and TL pottery dating indicates either an uninterrupted use of the tomb for at least two hundred years (1320–1120 BC), or a shorter continuous use (1320–1170 BC) followed by a reuse in the Geometric to Early Archaic periods.

The OSL dates obtained from the lowest course slabs of the Tomb A, just above the bedrock, provide further evidence for its use. The higher date (1660–1040 BC) fits well with the multiple occupancy and the dates of the pottery and the figurines. The lower date (1038–762 BC), however, does not overlap at all with the higher one. It indicates without a doubt that the tomb has been reopened sometime during the Sub-Mycenaean or/and the Geometric periods. Various reasons could have led to such a step, among which a new burial is the most probable. To this explanation points also the right femur collected in the upper stratum inside the tomb before the start of the excavation, with calibrated C-14 date

Please cite this article in press as: I. Liritzis, et al., Luminescence dating of stone wall, tomb and ceramics of Kastrouli (Phokis, Greece) Late Helladic settlement: Case study, Journal of Cultural Heritage (2018), https://doi.org/10.1016/j.culher.2018.07.009

810–760 BC [7]. Alternately, looting already in this early time cannot be excluded, although some kind of heroic cult would have been more in the spirit of what we know from other Mycenaean tombs, including those in the nearby Medeon and Delphi ([42], 133–135).

The OSL dates of the fortification wall indicate at least two or possibly even three phases. The earliest one (1395–1105 BC), covering practically the entire 14th–12th centuries, is in accordance with the pottery finds, which on typological/stylistic criteria are not earlier than 1370 BC. The other two dates (810–550 BC and 577–297 BC) overlap slightly for a quarter of a century and if they are correctly correlated they may indicate some major repairs on the wall during the second quarter of the 6th century BC. This would be the time immediately after the First Sacred War in Phokis, an event which may have triggered the need for rehabilitation or upgrade of the Kastrouli fort. If, however, they represent two distinctive events, they should be interpreted as two major interventions or repairs of the wall: one during the Archaic period and another, either in the Late Archaic or in the Classical periods. This does not come as a surprise since Archaic and Classical sherds have been reported on the surface of the Kastrouli site by Dasios ([4], 84) and Raptopoulos ([5], 1072). The obtained dates for ceramics and fortified stone wall and the tomb reinforce the Late Bronze age of the settlement and subsequent reuse, bearing in mind the error incurred with luminescence dating. The TL of ceramics was used for determination of the firing age but also in one case the firing temperature. The firing temperatures of most excavated ceramic fabric in the site which was analyzed by XRD and SEM has shown temperatures from 700 to 1100 °C ([43] in preparation). Poorly fired ceramics sherds have been visually noticed. The SLD version of OSL dating revealed and confirmed the reuse of the site. This reuse has been already supposed earlier by a C14 date 9th–8th c BC of femur bone from the tomb as well as from OSL of ceramic sherds scattered in the site of 12th, 7th and 5th c BC [7]. The limited amount of removed surface powder from the stone pieces however produced at least 4–5 aliquots per surface area of interest in each piece. The consistency of EDs and their credibility is strongly supported by the values of both the recycling ratios of the main measurements (naturally accrued dose), which lie within the range 0.93–0.99, and the recuperation, which is less than 8.1%.

The microdosimetry of stone and ceramics is a crucial issue; the shallow bedrock, the carved rocky background and the infill of sediments made the environmental gamma rays dose rate a painstaking task for evaluation. The radiation geometry has been met elsewhere and the age equation cannot be employed based on current softwares but in part individually calculated (see footnotes of Table 4).

The luminescence ages are concordant and expected when compared to the typology of implements and the fortified wall of a prior archaeological survey by our team as well as earlier rescue excavations.

6. Conclusion

The luminescence dating (OSL and TL) of ceramic and stone of the new settlement at Kastrouli central Greece has fulfilled the aims: (a) we have produced ages from the Hellenistic/Roman to Late Mycenean/Helladic times indicating that the site was reused by later people of whom at least the early Geometric ones were successors judging from the burial custom. Following the 9th c BC in the archaic, Classical and Hellenistic times the settlement was in use, and (b) provided a definite LBA destruction of the site. The fine grain quartz MAAD procedure of TL of ceramics was used and for the quartz presence in the limestone rock samples the SAR protocol for the dose determination. The dose rates were evaluated per each radiation component and the appropriate corrections for grain size attenuation, water uptake and fractional contribution in their geometrical setting. The firing temperature of one ceramic is low compared to the usual firing ranges in ancient ceramics. Although the incurred luminescence dating errors in the method is around 5–7% the application to a complex dosimetry situation and the investigation of the use of the settlement and the looted tomb on the obtained ages provided valuable information which gradually unfolds its life span and together with current analytical work sprang its importance as a little but major settlement in the periphery of the Mycenaean World of mainland Greece.

Acknowledgements

IL and AS thank the Ministry of Culture and the Ephoreia of Antiquities of Phokis for granting permission and collaboration. IL thanks Dr. A. Sarantopoulos of the National Meteorological Service for his kindness to provide meteorological data the period 1961–2018. Chemical measurements with SEM-EDS at Kalamata is fully acknowledged (c/o Prof N. Zacharias), as well as the drone orthophoto by D. Stefanakis. This dating project was made without any grant funding.

References

[1] T.E. Levy, T. Sideris, M. Howland, B. Liss, G. Tsokas, A. Stambolidis, E. Fikos, G. Vargemezis, P. Tsourlos, A. Georgopoulos, G. Papatheodorou, M. Garaga, D. Christodoulou, R. Norris, I. Rivera-Collazo, I. Liritzis, At-risk world heritage, cyber, and marine archaeology: The Kastrouli–Antikyra bay land and sea project, Phokis, Greece, chapter 9, in: T.E. Levy, I.W.N. Jones (Eds.), Cyber-Archaeology and Grand Narratives, One World Archaeology, © Springer International Publishing AG, 2018, pp. 141–230, http://dx.doi.org/10.1007/978-3-319-65693-9_9.
[2] E.H. Cline, 1177 B.C.: The Year Civilization Collapsed, Princeton University Press, Princeton, 2014.
[3] A. Sideris, I. Liritzis, B. Liss, M.D. Howland, T.E. Levy, At-risk cultural heritage: new excavations and finds from the Mycenaean site of Kastrouli, Phokis, Greece, Mediterr. Archaeol. Archaeom. 17 (1) (2017) 271–285.
[4] F. Dasios, Contribution to the topography of ancient Phokis, Fokika Khronika 4 (1992) 18–97 (in Greek).
[5] S. Raptopoulos, Mycenaean tholos tomb in Desfina of Phokis, Arkheologiko Ergo Thessalias kai Stereas Elladas 3 2009 (2012) 1071–1078 (in Greek).
[6] A. Sideris, I. Liritzis, Excavations and finds from the Mycenaean site of Kastrouli, Phokis, Greece. Second season – July 2017, Mediterr. Archaeol. Archaeom. 18 (2018) (forthcoming).
[7] I. Liritzis, Z. Jin, A. Fan, A. Sideris, A. Drivaliari, Late Helladic and later reuse phases of Kastrouli settlement (Greece): preliminary dating results, Mediterr. Archaeol. Archaeom. 16 (3) (2016) 245–250.
[8] I. Liritzis, G.S. Polymeris, N. Zacharias, Surface luminescence dating of 'Dragon Houses' and Armena Gate at Styra (Euboea, Greece), Mediterr. Archaeol. Archaeom., Spec. Issue 10 (3) (2010) 65–81 (D. Keller, guest editor).
[9] I. Liritzis, A.K. Singhvi, J.K. Feathers, G.A. Wagner, A. Kadereit, N. Zacharias, S.-H. Li, Luminescence Dating Protocols and Dating Range, in: Archaeology, Anthropology and Geoarchaeology: An Overview, Springer Briefs in Earth System Sciences, 2013, pp. 5–20 http://link.springer.com/content/pdf/10.1007/978-3-319-00170-8.pdf.
[10] I. Liritzis, A. Vafiadou, Surface luminescence dating of some Egyptian monuments, J. Cult. Herit. 16 (2015) 134–150.
[11] I. Liritzis, V. Aravantinos, G.S. Polymeris, N. Zacharias, I. Fappas, G. Agiamarniotis, I.K. Sfampa, A. Vafiadou, G. Kitis, Witnessing prehistoric Delphi by Luminescence dating, C. R. Palevol 14 (2015) 219–232.
[12] D.W. Zimmerman, Thermoluminescence dating using fine grains from pottery, Archaeometry 13 (1971) 29–52.
[13] L. Bøtter-Jensen, E. Bulur, G.A.T. Duller, A.S. Murray, Advances in luminescence instrument systems, Radiat. Meas. 32 (2000) 523–528.
[14] G. Kitis, N.G. Kiyak, G.S. Polymeris, Temperature lags of luminescence measurements in a commercial luminescence reader, Nucl. Instrum. Methods Phys. Res. B 359 (2015) 60–63.
[15] M.J. Aitken, Thermoluminescence Dating, Academic Press, London, 1985.
[16] M.J. Aitken, An Introduction to Optical Dating: the Dating of Quaternary Sediments by the Use of Photon-stimulated Luminescence, Oxford Science Publications, Oxford, 1998.
[17] G.A. Wagner, Age Determination of Young Rocks and Artifacts: Physical and Chemical Clocks in Quaternary Geology and Archaeology, Springer–Verlag, Berlin Heidelberg, 1998.
[18] M.S. Murray, A.G. Wintle, Luminescence dating of quartz using an improved single – aliquot regenerative – dose protocol, Radiat. Meas. 32 (2000) 57–73.
[19] D. Banerjee, A.S. Murray, L. Bøtter-Jensen, A. Lang, Equivalent dose estimation using a single aliquot of polymineral fine grains, Radiat. Meas. 33 (2001) 73–94.
[20] I. Liritzis, A. Drivaliari, G.S. Polymeris, C. Katagas, New quartz technique for OSL dating of limestones, Mediterr. Archaeol. Archaeom. 10 (1) (2010) 81–87.

Please cite this article in press as: I. Liritzis, et al., Luminescence dating of stone wall, tomb and ceramics of Kastrouli (Phokis, Greece) Late Helladic settlement: Case study, Journal of Cultural Heritage (2018), https://doi.org/10.1016/j.culher.2018.07.009

[21] G.S. Polymeris, N.G. Kiyak, D.K. Koul, G. Kitis, The firing temperature of pottery from ancient Mesopotamia, Turkey, using luminescence methods: a case study for different grain size fractions, Archaeometry 56 (5) (2014) 805–817.
[22] G.S. Polymeris, A. Sakalis, D. Papadopoulou, G. Dallas, G. Kitis, N.C. Tsirliganis, Firing Temperature of pottery using TL and OSL techniques, Nucl. Instrum. Methods Phys. Res. A 580 (2007) 747–750.
[23] J. Sanjurjo-Sanchez, M. Gomez-Heras, G.S. Polymeris, Estimating maximum temperatures attained during fires in building stoneworks by thermoluminescence: a case study from Uncastillo, Saragossa (Spain), Mediterr. Archaeol. Archaeom. 13 (3) (2013) 145–153.
[24] J. Sanjurjo-Sanchez, J.L. Montero Fenollós, G.S. Polymeris, Technological aspects of Mesopotamian Uruk pottery: estimating firing temperatures using mineralogical methods, thermal analysis and luminescence techniques, Archaeol. Anthropol. Sci. 10 (4) (2018) 849–864.
[25] G.S. Polymeris, Thermally assisted OSL (TA-OSL) from various luminescence phosphors; an overview, Radiat. Meas. 90 (2016) 145–152.
[26] G.S. Polymeris, A.E. Erginal, N.G. Kiyak, A comperative morphology, compositional as well as TL study of Bozcaada (Tenedos) and Şile aeolianites, Turkey, Mediterr. Archaeol. Archaeom. 12 (2) (2012) 117–131.
[27] A.S. Murray, A.G. Wintle, The single aliquot regenerative dose protocol: potential for improvements in reliability, Radiat. Meas. 37 (2003) 377–381.
[28] I. Liritzis, 110 °C quartz peak: a new normalization factor, Ancient TL 11 (1980) 6–7.
[29] D.K. Koul, Role of alkali ions in limiting the capacity of the 110 °C peak of quartz to remember the firing temperature, Appl. Radiat. Isotopes 64 (2006) 110–115.
[30] G.S. Polymeris, D. Afouxenidis, S. Raptis, I. Liritzis, N.C. Tsirliganis, G. Kitis, Relative response of TL and component-resolved OSL to alpha and beta radiations in annealed sedimentary quartz, Radiat. Meas. 46 (2011) 1055–1064.
[31] J.R. Prescott, J.T. Hutton, Cosmic ray and gamma ray dosimetry for TL and ESR, Nucl. Tracks Radiat. Meas. 14 (1988) 223–227.
[32] E. Storm, E.I. Israel, Photon Cross-Sections from 0.601 to 100 MeV for Elements 1 Through 100, LA-3753, University of California, United States, 1967 (Web. doi:10.2172/4583232).
[33] R.D. Evans, X- and γ-ray interactions, Radiation Dosimetry, in: F. Attix, W.C. Roesch (Eds.), Fundamentals, Volume I, second ed., Academic Press, New York/London, 1968, pp. 93–155.
[34] R.D. Evans, The Atomic Nucleus, McGraw-Hill, New York, 1955.
[35] I. Liritzis, K. Stamoulis, C. Papachristodoulou, K.G. Ioannides, A re-evaluation of radiation dose rate conversion factors, Mediterr. Archaeol. Archaeom. Spec., 13 (3) (2013) 1–15.
[36] M.-E. Chovalopoulou, A. Bertsatos, S.K. Manolis, Identification of skeletal remains from a Mycenaean burial in Kastrouli-Desfina, Mediterr. Archaeol. Archaeom. 17 (1) (2017) 265–269.
[37] S. Deger-Jalkotzy, M. Zavadil, LH III C Chronology and Synchronisms: Proceedings of the International Workshop held at the Austrian Academy of Sciences at Vienna, May 7th and 8th, (Wien 2001), Veröffentlichungen der Mykenischen Kommission, Bd. 20; Denkschriften (Österreichische Akademie der Wissenschaften. Philosophisch-Historische Klasse), 2001 (Bd. 310).
[38] M.H. Wiener, The Absolute Chronology of Late Helladic IIIA2 Revisited, BSA 98, 2003, pp. 239–250.
[39] S. Vitale, The LH IIIB – LH IIIC Transition on the Mycenaean Mainland. Ceramic Phases and Terminology, Hesperia 75 (2006) 177–204.
[40] D.A. Aston, The LH IIIA2 – IIIB transition: the Gurob and Saqqara evidence reassessed, in: W. Gauss, M. Lindblom, R.A.K. Smith, J.C. Wright (Eds.), Our Cups Are Full: Pottery and Society in the Aegean Bronze Age, Oxford, Archaeopress, 2011, pp. 1–12.
[41] M.B. Toffolo, A. Fantalkin, I.S. Lemos, R.C.S. Felsch, W.-D. Niemeier, G.D.R. Sanders, Towards an absolute chronology for the Aegean Iron Age: new radiocarbon dates from Lefkandi, Kalapodi and Corinth, PLoS ONE 8 (12) (2013), e83117, http://dx.doi.org/10.1371/journal.pone.0083117.
[42] C. Antonaccio, An Archaeology of Ancestors. Hero and Tomb Cult in Early Greece, London, Rowman & Littlefield Publ. Inc., 1993.
[43] I. Liritzis, N. Zacharias, I. Iliopoulos, E. Palamara, V. Xanthopoulou, A. Sideris, A. Vafiadou, A detailed archaeometric analysis for characterization and provenance of ceramic fabric and local clays from Late Helladic Kastrouli (Central Greece), 2018 (results to be submitted for publication).

Please cite this article in press as: I. Liritzis, et al., Luminescence dating of stone wall, tomb and ceramics of Kastrouli (Phokis, Greece) Late Helladic settlement: Case study, Journal of Cultural Heritage (2018), https://doi.org/10.1016/j.culher.2018.07.009